

# Collision of Domain Walls in asymptotically Anti de Sitter spacetime

Yu-ichi Takamizu<sup>1\*</sup> and Kei-ichi Maeda<sup>1,2,3†</sup>

<sup>1</sup> *Department of Physics, Waseda University, Okubo 3-4-1, Shinjuku, Tokyo 169-8555, Japan*

<sup>2</sup> *Advanced Research Institute for Science and Engineering,*

*Waseda University, Okubo 3-4-1, Shinjuku, Tokyo 169-8555, Japan*

<sup>3</sup> *Waseda Institute for Astrophysics, Waseda University, Okubo 3-4-1, Shinjuku, Tokyo 169-8555, Japan*

(Dated: February 1, 2008)

We study collision of two domain walls in 5-dimensional asymptotically Anti de Sitter spacetime. This may provide the reheating mechanism of an ekpyrotic (or cyclic) brane universe, in which two BPS branes collide and evolve into a hot big bang universe. We evaluate a change of scalar field making the domain wall and can investigate the effect of a negative cosmological term in the bulk to the collision process and the evolution of our universe.

PACS numbers: 98.80.Cq

## I. INTRODUCTION

The theory of inflation not only resolves the key theoretical problems of a big bang theory such as the flatness and the horizon problems [1, 2], but also seems to be confirmed by recent observational data on CMB [3]. However, it is still unclear what is the inflaton in a fundamental unified theory such as string/M-theory. So far, there has not been found a convincing model, although we may have several possible links [4, 5].

While, a new paradigm on the early universe, the so-called brane world has been proposed [6, 7]. Such speculation has been inspired by recent developments in string/M-theory [8, 9, 10]. There has been tremendous work on this scheme of dimensional reduction [11, 12], where ordinary matter fields are confined on a lower-dimensional hypersurface, while only gravitational field propagates throughout all of spacetime. Among such dimensional reduction scenarios, Randall and Sundrum (RS) [12] proposed a new model where four-dimensional Newtonian gravity is recovered at low energies even without compact extra dimensions. Based on such a new world picture, many cosmological scenarios have been studied [13, 14, 15]. See also recent reviews [16, 17, 18, 19]. We have found some deviations from standard cosmology by modifications of 4-dimensional Einstein equations on the brane [20], even for the case that there is a scalar field in bulk [21].

In such a brane world scenario, for resolving the above-mentioned key theoretical problems in the big bang theory, a new idea of cosmological model has been proposed, which is called the ekpyrotic scenario or the cyclic universe scenario [22, 23]. It could be an alternative to an inflationary scenario. Since it is not only motivated by such fundamental unified theory but also may resolve the above mentioned key cosmological problems, it would be very attractive.

This scenario is based on a collision of two cold branes. The universe starts with a cold, empty, and nearly BPS ground state, which contains two parallel branes at rest. The two branes approach each other and then collide. The energy is dissipated on the brane and the big bang universe starts. The BPS state is required in order to retain a supersymmetry in a low-energy 4-dimensional effective action. The visible and hidden branes are flat and are described by a Minkowski spacetime, but the bulk is warped along the fifth dimension.

There has been much discussion about density perturbations to see whether this scenario is really a reliable scenario for the early universe [24, 25, 26, 27]. It has been shown that the initial spectrum seems not to be produced as a scale invariant one. So this is the weakness of this scenario. However, it may turn out that we find other wayout to produce a scale invariant fluctuation. Then, it is necessary to analyze the other important process in this scenario, e.g. the reheating process, in detail. For the work about the collision of branes, there has been some studies by [28, 29] with using the brane approximated as the delta function. In the analysis using a delta function, the microscopic processes in collision such as dissipation of matter field and reheating of the universe can not be described. Even though there are some works on [30], the reheating mechanism itself has not been so far investigated in detail. So the purpose of our work is to construct a consistent brane collision model and to analyze its reheating process.

With such analysis, we may find how we can recover the hot big bang universe after the collision of branes. In our previous work (paper I) [31], we proposed a new reheating mechanism in the ekpyrotic universe, such as a quantum creation of particles confined on the brane at the collision of two branes. As a thick brane, we could adopt a domain wall model constructed by a bulk scalar field and analyze the collision of two moving domain walls in a 5-dimensional bulk spacetime. In the paper I, we consider the simplest situation such that two domain walls collide in a given background spacetime, i.e. the five-dimensional (5D) Minkowski spacetime. As shown by several authors [32, 33, 34, 35], the results highly de-

\*Electronic address: takamizu@gravity.phys.waseda.ac.jp

†Electronic address: maeda@gravity.phys.waseda.ac.jp

pend on the incident velocity  $v$  of the walls. We have shown the time evolution of colliding two domain walls in the paper I, which confirms the previous works. For a sufficiently large velocity, e.g.  $v \gtrsim 0.25$ , it is shown that a kink and antikink will just bounce off once, because there is no time to exchange the energy during the collision. For a lower velocity, we find multiple bounces when they collide. For example, we find the bounce occurs once for  $v = 0.4$ , while it does twice for  $v = 0.2$ . We also find many bounce solutions for other incident velocities, as shown in Appendix B of [31] (see also [32]). The number of the bounces sensitively depends on the incident velocity. A set of the values of  $v$  which give the same number of bounce forms a fractal structure in the  $v$ -space as shown Fig. 6 of [32]. Then, we evaluate a production rate of particles confined to the domain wall. As a result, the energy density of created particles is given as  $\rho \approx 20\bar{g}^4 N_b m_\Phi^4$  where  $\bar{g}$  is a coupling constant of particles to a domain-wall scalar field,  $N_b$  is the number of bounces at the collision and  $m_\Phi$  is a fundamental mass scale of the domain wall. It does not depend on the width  $d$  of the domain wall, although the typical energy scale of created particles is given by  $\omega \sim 1/d$ . The reheating temperature is evaluated as  $T_R \approx 0.88 \bar{g} N_b^{1/4}$ . In order to have the baryogenesis at the electro-weak energy scale, the fundamental mass scale is constrained as  $m_\eta \gtrsim 1.1 \times 10^7$  GeV for  $\bar{g} \sim 10^{-5}$ . For such an energy scale, we may find a sufficiently hot universe after collision of domain walls.

In order to study whether such a reheating process is still efficient in more reliable cosmological models, we have to include the curvature effect. In particular, some brane universe are discussed with a negative cosmological constant [12] Hence, we study here how gravitational effects change our previous results. In order to investigate such an effect, we have not only to investigate the collision of domain walls in a curved spacetime, but also to solve the spacetime by use of the 5D Einstein equations. Inspired by the RS brane model, we include a potential of the scalar field which provides an effective negative cosmological constant in a bulk spacetime.

We first set up the initially moving two domain walls, each of which is obtained by boosting an exact static domain wall solution [36] (§II). Although this solution is obtained in the four dimensions, it is easy to extend it to the 5D one. We then solve the 5D Einstein equations and the dynamical equation for a scalar field to analyze collision of thick walls in asymptotically AdS spacetime (§III). The concluding remarks follow in §IV.

We use the unit of  $c = \hbar = 1$ .

## II. COLLISION OF TWO DOMAIN WALLS

### A. Basic Equations

We study collision of two domain walls in 5D spacetime. To construct a domain wall structure, we adopt

a 5D real scalar field  $\Phi$  with an appropriate potential  $V(\Phi)$ , which minimum value is negative. This potential gives an asymptotically anti-de Sitter (AdS) spacetime just as the RS brane model.

Since we discuss the collision of two parallel domain walls, the scalar field is assumed to depend only on a time coordinate  $t$  and one spatial coordinate  $z$ . The remaining three spatial coordinates are denoted by  $\mathbf{x}$ . For numerical analysis, we use dimensionless parameters and variables, which are rescaled by the mass scale  $m_\Phi$ , which is defined by the vacuum expectation value at a local minimum as  $\Phi_0 = m_\Phi^{3/2}$ , as

$$\tilde{t} = m_\Phi t, \quad \tilde{z} = m_\Phi z, \quad \tilde{\Phi} = \frac{\Phi}{m_\Phi^{3/2}}. \quad (2.1)$$

In what follows, we drop the tilde in dimensionless variables for brevity.

It is possible to choose coordinates such that the bulk metric has the “2D conformal gauge”, i.e.

$$ds^2 = e^{2A(t,z)}(-dt^2 + dz^2) + e^{2B(t,z)}d\mathbf{x}^2. \quad (2.2)$$

This gauge choice also makes the initial setting easy when we construct moving domain walls by use of the Lorentz boost.

In this gauge, the 5D Einstein equations and the dynamical equation for a scalar field are split into three dynamical equations;

$$\begin{aligned} \ddot{A} &= A'' + 3\dot{B}^2 - 3B'^2 - \kappa_5^2(\dot{\Phi}^2 - \Phi'^2 + \frac{1}{3}e^{2A}V(\Phi)), \\ \ddot{B} &= B'' - 3\dot{B}^2 + 3B'^2 + \frac{2}{3}\kappa_5^2e^{2A}V(\Phi), \\ \ddot{\Phi} &= \Phi'' - 3\dot{B}\dot{\Phi} + 3B'\Phi' - \frac{1}{2}e^{2A}V'(\Phi), \end{aligned} \quad (2.3)$$

plus two constraint equations;

$$\begin{aligned} \dot{B}B' - A'\dot{B} - \dot{A}B' + \dot{B}' &= -\frac{2}{3}\kappa_5^2\dot{\Phi}\Phi', \\ 2B'^2 + B'' - A'B' - \dot{A}\dot{B} - \dot{B}^2 &= -\frac{1}{3}\kappa_5^2(\dot{\Phi}^2 + \Phi'^2 + e^{2A}V(\Phi)), \end{aligned} \quad (2.4)$$

where a dot ( $\dot{\phantom{x}}$ ) and a prime ( $\prime$ ) denote  $\partial/\partial t$  and  $\partial/\partial z$ , respectively.

These are our basic equations. Before solve them numerically, we have to set up our initial data, which satisfies the constraint equations (2.4).

### B. Domain Wall Solution

For an initial configuration of a domain wall, we use an exact static solution given by [36]. They assume a scalar field  $\Phi$  with a potential

$$V(\Phi) = \left(\frac{\partial W}{\partial \Phi}\right)^2 - \frac{8}{3}\kappa_5^2 W^2, \quad (2.5)$$

where

$$W \equiv \frac{1}{d} \left( \Phi - \frac{1}{3} \Phi^3 - \frac{2}{3} \right) \quad (2.6)$$

is a superpotential, and  $\kappa_5^2$  and  $d$  are the five dimensional gravitational constant and the thickness of a domain wall, respectively. The potential minima are located at  $\Phi = \pm 1$  in the range of  $|\Phi| \lesssim 5$  (see Fig. 1). The potential shape is similar to a double-well potential, but it is asymmetric. The minimum value at  $\Phi = 1$  vanishes, while that at  $\Phi = -1$  is negative. With this potential, we can obtain analytically an exact solution for two colliding domain walls as follows.

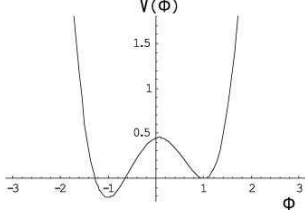


FIG. 1: The scalar field potential  $V(\Phi)$  is plotted where  $d = \sqrt{2}$ ,  $\kappa_5 = 0.3$ . This potential behaves like a double-well potential for  $|\Phi| < 5$ , except that one of its two minima has a negative value. On the other hand, for  $|\Phi| > 5$ , this potential behaves differently from a double-well potential, that is  $V(\Phi)$  rapidly falls into  $-\infty$ .

First, we show a static domain wall solution with this potential. A kink solution of a scalar field ( $K$ ) is described as

$$\Phi_K(y) = \tanh \left( \frac{y}{d} \right), \quad (2.7)$$

and the metric of 5D spacetime is

$$ds^2 = e^{2A_K(y)} (-dt^2 + d\mathbf{x}^2) + dy^2, \quad (2.8)$$

with

$$A_K(y) = -\frac{4}{9} \kappa_5^2 \left\{ \ln \left[ \cosh \left( \frac{y}{d} \right) \right] + \frac{\tanh^2(y/d)}{4} - \frac{y}{d} \right\}. \quad (2.9)$$

Since this exact solution is not given in our gauge, we have used a new coordinate  $y$ , which will be associated with  $z$  later.

This metric approaches that of the AdS spacetime in one asymptotic region ( $y \ll -1$ ), i.e.

$$e^{2A_K} \rightarrow e^{-2k|y|} \quad \text{as } y \rightarrow -\infty, \quad (2.10)$$

with

$$k = \frac{8\kappa_5^2}{9d}. \quad (2.11)$$

While it becomes a flat Minkowski space in another asymptotic region ( $y \gg 1$ ), i.e.

$$e^{2A_K} \rightarrow e^{2A_\infty} \quad \text{as } y \rightarrow \infty, \quad (2.12)$$

with

$$A_\infty = \frac{4}{9} \kappa_5^2 \left( \log 2 - \frac{1}{4} \right). \quad (2.13)$$

We depict the behaviour of metric function  $\exp[A_K(y)]$  in Fig. 2.

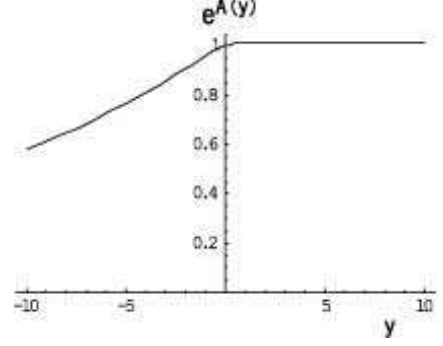


FIG. 2: The metric component of the exact solution for a static domain wall [36] is plotted where we set  $d = \sqrt{2}$  and  $\kappa_5 = 0.3$ . This spacetime approaches Minkowski space because  $A_K \rightarrow A_\infty$  (a constant), while it becomes asymptotically AdS because  $A_K \rightarrow -k|y|$  as  $y \rightarrow -\infty$ , where  $k = 8\kappa_5^2/9d$ .

By reflecting the spatial coordinate  $y$ , we also find an antikink solution ( $\bar{K}$ ) as  $\Phi_{\bar{K}}(y) = \Phi_K(-y) = -\Phi_K(y)$ . The corresponding metric of this antikink solution is also obtained by reflection of  $y$ -coordinate, i.e.  $A_{\bar{K}}(y) = A_K(-y) = -A_K(y)$ .

In order to describe this solution under our gauge condition (2.2), that is, in the  $(t, z)$  frame, we should transform the present  $(t, y)$  coordinates (Eq.(2.8)) into the  $(t, z)$  ones (Eq.(2.2)) by defining the coordinate  $z$  as

$$z = \int e^{-A_K(y)} dy. \quad (2.14)$$

This integration will be performed numerically to find initial data of collision of two domain walls.

### C. Moving Domain Wall

When a domain wall moves with constant speed  $v$  in the fifth direction  $z$ , we can obtain the corresponding solution by boosting a static kink solution ( $K$ ) as

$$\Phi_v(z, t) = \tanh \left[ \frac{1}{d} y^*(\gamma(z - vt)) \right], \quad (2.15)$$

where  $y^*$  and  $z^*$  are comoving coordinates of a domain wall, and  $y^*(z^*)$  is obtained by the inverse transformation of Eq. (2.14). The Lorentz transformation gives  $z^* = \gamma(z - vt)$  where  $\gamma = 1/\sqrt{1 - v^2}$  is the Lorentz factor. We have assumed that the center of a domain wall is initially located at  $z = 0$ .

The corresponding metric is easily obtained by Lorentz boost. Because of the Lorentz invariance in our 2D conformal gauge, i.e.,  $-dt^{*2} + dz^{*2} = -dt^2 + dz^2$ , we find

$$ds_{2D}^2 = \exp[2A_K(\gamma(z - vt))]( -dt^2 + dz^2 ), \quad (2.16)$$

where  $A_K(z^*) = A_K(y^*(z^*))$ . The function  $A_K(y)$  is given by Eq. (2.9). The center of a domain wall ( $z^* = 0$ ) moves as  $z = vt$  in our  $(t, z)$ -coordinate frame. Then we regard that the metric describes a spacetime with a domain wall moving with constant speed  $v$  in the  $z$  direction as well as a scalar field  $\Phi$  does so.

In order to discuss collision of two moving domain walls, we first have to set up its initial data. Using Eqs. (2.15) and (2.16), we can construct an initial data for two moving domain walls as follows. Provide a kink solution at  $z = -z_0$  and an antikink solution at  $z = z_0$ , which are separated by a large distance and approaching each other with the same speed  $v$ . We then obtain the following initial data;

$$\begin{aligned} \Phi(z, 0) &= \Phi_v(z + z_0, 0) - \Phi_{-v}(z - z_0, 0) - 1, \\ A(z, 0) &= A_v(z + z_0, 0) - A_{-v}(z - z_0, 0) - A_\infty, \end{aligned} \quad (2.17)$$

where  $A_\infty$  is the constant value given by Eq. (2.13). The initial values of  $\dot{\Phi}$  and  $\dot{A}$  are also given by

$$\begin{aligned} \dot{\Phi}(z, 0) &= \dot{\Phi}_v(z + z_0, 0) - \dot{\Phi}_{-v}(z - z_0, 0), \\ \dot{A}(z, 0) &= \dot{A}_v(z + z_0, 0) - \dot{A}_{-v}(z - z_0, 0). \end{aligned} \quad (2.18)$$

Obviously, we set  $A = B$  and  $\dot{A} = \dot{B}$  at initial.

The spatial separation between two walls is given by  $2z_0$ , and as long as the separation distance is much larger than the thickness of the wall ( $z_0 \gg d$ ), the initial conditions (2.17) and (2.18) give a good approximation for two moving domain walls. Using these initial values, we solve the dynamical equation (2.3) numerically. The results will be shown in the next section.

### III. TIME EVOLUTION OF COLLIDING DOMAIN WALLS

We use a numerical approach to solve the dynamical equations (2.3) for the colliding domain walls. We adopt a numerical method similar to one used in [31]. The difference is found in a boundary conditions. We impose the Dirichlet boundary condition for the scalar field, which is the same as the paper I, while the Neumann boundary condition is used for the metric as  $A'(z) = -k\gamma e^{A(z)}$ , which is derived from the asymptotic form of the metric, i.e.,  $e^{A(z)} \rightarrow 1/(k(\gamma|z| + 1))$  as  $|z| \rightarrow \infty$ .

We have three free parameters in our model, i.e. a wall thickness  $d$ , an initial wall velocity  $v$ , and a warp factor  $k$  (or the gravitational constant  $\kappa_5$ ). Two of them ( $d, k$  (or  $\kappa_5$ )) are fundamental because they appear in the theory. In the paper I, we studied the collision of two

domain walls in the fixed Minkowski background [32], where we had two free parameters  $d$  and  $v$ . So, including the gravitational back reaction, we investigate how  $\kappa_5$  (or  $k$ ) changes the previous results. In what follows, fixing the value of  $d$ , i.e.  $d = \sqrt{2}$ , we show our results.

#### A. Time Evolution of Scalar Field $\Phi$

First let us set  $\kappa_5 = 0$  (or  $k = 0$ ), that is the case of Minkowski background spacetime. Although the scalar field potential is slightly different from that in the paper I, the result is exactly the same. This simulation also gives a check of our numerical code.

Next we perform our simulation for  $\kappa_5 \neq 0$ . For a small value of  $\kappa_5$ , i.e.,  $\kappa_5 \lesssim 0.05$  (equivalently  $k \lesssim 1.57 \times 10^{-3}$  or  $m_\Phi \lesssim (0.05)^{2/3} m_5 \approx 0.136 m_5$ ), the collision process is very similar to the case of the Minkowski background. Setting the initial velocity  $v = 0.4$ , we show our numerical results for  $\kappa_5 = 0.05$  in Figs. 3 and 4. The evolution of  $\Phi$  is depicted in Fig. 3, while that of the energy density is shown in Fig. 4.

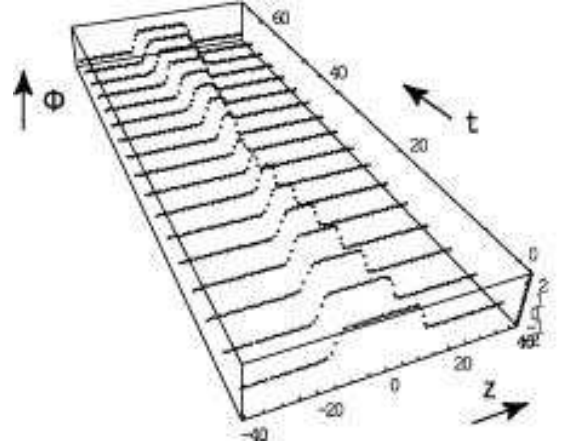


FIG. 3: Collision of two domain walls where the initial velocity  $v = 0.4$ . The time evolution of the scalar field  $\Phi$  is shown from  $t = 0$  to 70. The collision occurs once around  $t = 31$ . We set  $d = \sqrt{2}$ ,  $\kappa_5 = 0.05$ . This process is similar to the Minkowski case,  $\kappa_5 = 0$ .

The energy density of the scalar field is given by

$$\rho_\Phi = e^{-2A} (\dot{\Phi}^2 + \Phi'^2) + V(\Phi). \quad (3.1)$$

We find some peaks in the energy density, by which we define the positions of moving walls ( $z = \pm z_W(t)$ ). If a domain wall is symmetric, its position is defined by  $\Phi(z) = 0$ . However, in more general situation, just as in the present case that the scalar field is oscillating around some moving point, it may be natural to define the position of a domain wall by the maximum point of its energy density.

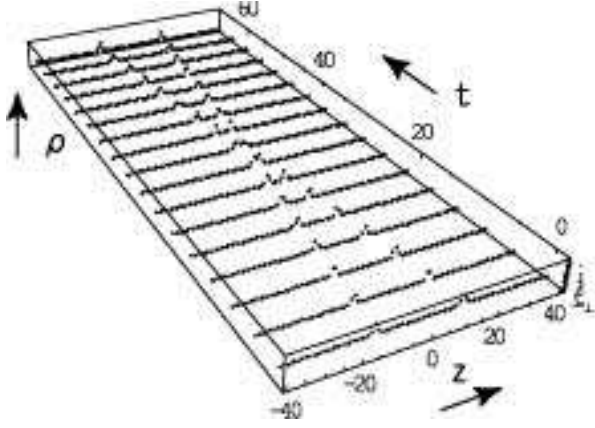


FIG. 4: The time evolution of scalar field energy density in the case of Fig. 3. The maximum point of  $\rho_\Phi$  defines the position of a wall ( $z = z_W(t)$ ).

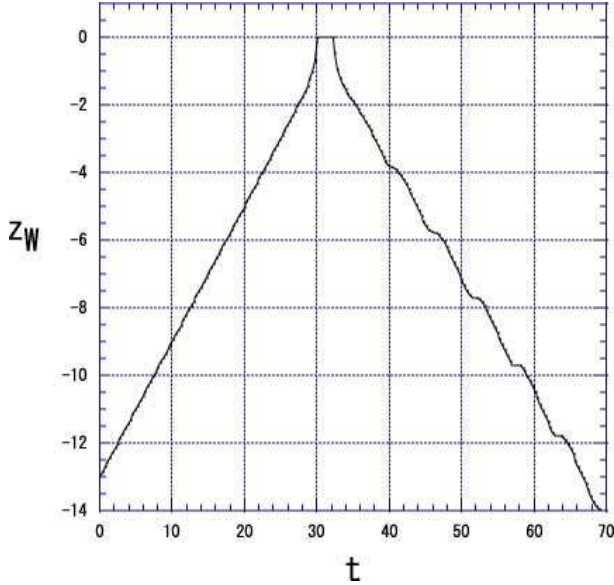


FIG. 5: Time evolution of the position of one brane  $z = z_W$  which starts to move at  $z = -13$  with a constant speed  $v = 0.4$ . We set  $d = \sqrt{2}$ ,  $\kappa_5 = 0.05$ .

Fig. 5 denotes the position of brane  $z = z_W(t)$  with respect to  $t$ . The brane moves with constant speed  $v = 0.4$  toward the collision point  $z = 0$ , and collide, then recede to the boundary. We also find small oscillation around a uniform motion after collision.

Since we assume that we are living on one domain wall, we are interested in a particle  $\psi$  confined on the domain wall. If a particle  $\psi$  is coupled with a 5-D scalar field  $\Phi$ , which is responsible for the domain wall, we expect quantum production of  $\psi$ -particles at collision of domain walls. This is because the value of the scalar field  $\Phi$  on the domain wall changes with time. This fact may play an important role in a reheating mechanism [31]. Once

we find the solution of colliding domain walls, we know the time evolution of a scalar field on the domain wall, and we can evaluate production rate.

At the position of a domain wall, the induced metric is given as

$$ds^2 = -d\tau^2 + a^2(\tau)d\mathbf{x}^2, \quad (3.2)$$

where proper time is determined as

$$\tau = \int e^{A_W} dt, \quad (3.3)$$

and the scale factor is

$$a(\tau) = e^{B_W(\tau)}. \quad (3.4)$$

$A_W$  and  $B_W$  are evaluated on the brane, i.e.,  $A_W = A(t, z_W(t))$  and  $B_W = B(t, z_W(t))$ . The Hubble parameter of the brane universe is defined by

$$H(\tau) \equiv \frac{1}{a} \frac{da}{d\tau} \Big|_{z=z_W} = \frac{dB_W}{d\tau} = e^{-A_W} \dot{B}_W(\tau). \quad (3.5)$$

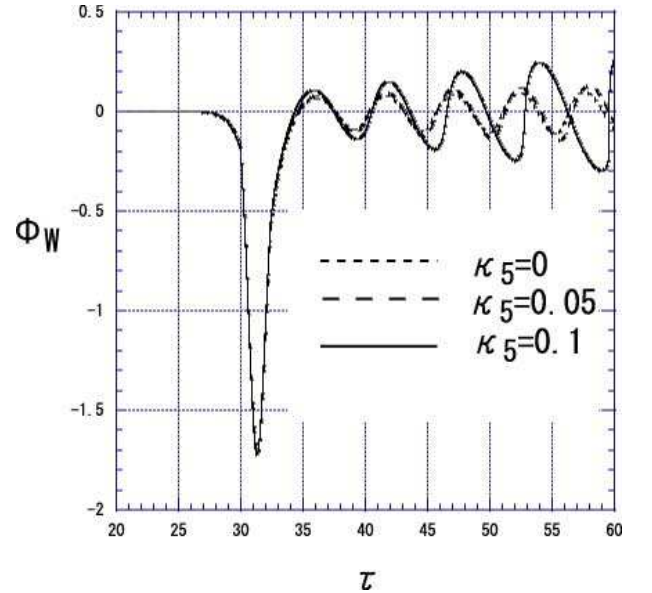


FIG. 6: Time evolution of a scalar field on the moving wall with  $v = 0.4$ ,  $d = \sqrt{2}$ . We set  $\kappa_5 = 0, 0.05, 0.1$ . The value of the scalar field on the wall is defined by  $\Phi_W = \Phi(t, z_W(t))$ , where  $z_W(t)$  is the position of the wall. The time of period of oscillation gets slightly longer and the amplitude is a little bit larger as  $\kappa_5$  increases.

For  $v = 0.4$ , we depict the time evolution of  $\Phi_W$  on one moving wall for different values of  $\kappa_5$  in Figs. 6 and 7. The feature of collision is similar, but the behaviour of a scalar field on the moving wall after collision is different for each  $\kappa_5$ .

We summarize our numerical results for each value of  $\kappa_5$  in order.

(i)  $\kappa_5 = 0.01$

For a small value of  $\kappa_5$ , e.g.,  $\kappa_5 = 0.01$  (equivalently  $k \sim 6.29 \times 10^{-5}$  or  $m_\Phi \sim 0.0464m_5$ ), the result is almost the same as the case of the Minkowski background, in which case we find one bounce point, which corresponds to a crossing point in Fig. 4, and then the oscillations around  $\Phi_W = 0$  follow (see the dotted line in Fig. 6). This oscillation is explained by using a perturbation analysis in Minkowski spacetime [31]. We have found one stable oscillation mode around the kink solution. This oscillation appears by excitation of the system at collision.

(ii)  $\kappa_5 = 0.05$

As increasing the value of  $\kappa_5$  slightly larger, for example  $\kappa_5 = 0.05$ , (equivalently for  $k \sim 1.57 \times 10^{-3}$  or  $m_\Phi \sim 0.136m_5$ ), the time evolution of  $\Phi_W$  slightly changes. In Fig. 6, just as the case of  $\kappa_5 = 0$ , we find one bounce and successive oscillations. However, the period of oscillation is slightly longer and the amplitude gets a little bit larger as  $\kappa_5$  increases.

(iii)  $\kappa_5 = 0.15$

For  $\kappa_5 = 0.15$ , (equivalently  $k \sim 1.41 \times 10^{-2}$  or  $m_\Phi \sim 0.282m_5$ ), the behaviour of this oscillation changes drastically. After several oscillations, the scalar field leaves  $\Phi_W = 0$  as shown in Fig. 7. The numerical simulation eventually breaks down because all variables diverge.

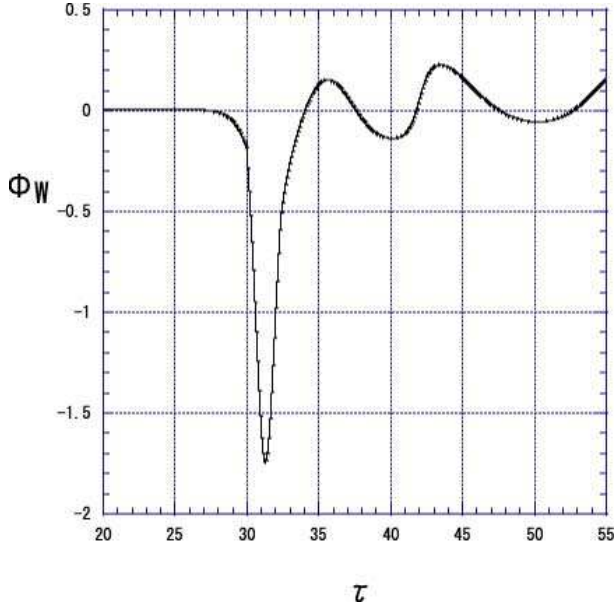


FIG. 7: Time evolution of a scalar field on the moving wall for  $v = 0.4$ ,  $d = \sqrt{2}$ ,  $\kappa_5 = 0.15$ . The value of the scalar field is given by  $\Phi_W = \Phi(t, z_W(t))$ , where  $z_W(t)$  is the position of the wall.  $\Phi_W$  goes out of oscillation phase 0 at  $\tau \sim 55$  and then numerical simulation stops.

(iv)  $\kappa_5 > 0.15$

For the larger values of  $\kappa_5$  than 0.15, the time to appear-

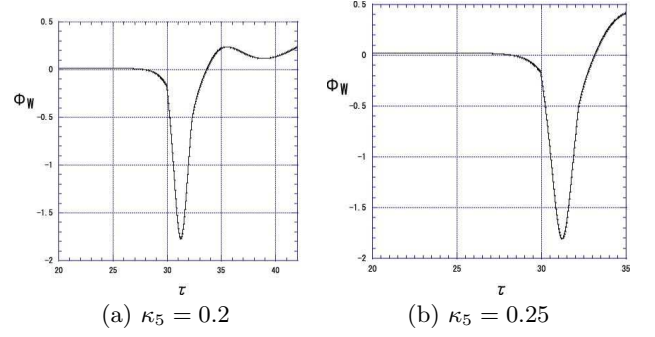


FIG. 8: Time evolution of the scalar field  $\Phi_W$  for  $v = 0.4$ ,  $d = \sqrt{2}$ , setting (a)  $\kappa_5 = 0.2$  and (b)  $\kappa_5 = 0.25$ . The numerical simulation breaks down when (a)  $\tau \sim 42$  and (b)  $\tau \sim 35$ , respectively.

ance of singularity becomes shorter, that is, contrary to the case of  $\kappa_5 \lesssim 0.15$ , the scalar field after collision does not oscillate but leave  $\Phi_W = 0$  soon. The time evolution of  $\Phi_W$  is shown in Fig. 8, for  $\kappa_5 = 0.2$  ( $k = 2.51 \times 10^{-2}$ ) and  $\kappa_5 = 0.25$  ( $k = 3.93 \times 10^{-2}$ ).

The metric component  $A$  at  $z = 0$  also diverges as shown in Fig 9. It is not a coordinate singularity, but a curvature singularity. In order to show it, we calculate the so-called Kretschmann invariant scalar, which is the simplest scalar invariant quadratic in the Riemann tensor, and is defined as

$$R^{abcd}R_{abcd} = e^{-4A} \left[ 3(\ddot{B} + \dot{B}^2 - \dot{A}\dot{B} - A'B')^2 - 3(A'\dot{B} + \dot{A}B' - \dot{B}' - \dot{B}B')^2 + (\ddot{A} - A'')^2 + 3(B'^2 - \dot{B}^2)^2 + 3(B'' + B'^2 - \dot{A}\dot{B} - A'B')^2 \right]. \quad (3.6)$$

In Fig. 9(b), we depict the time evolution of the Kretschmann scalar at the origin  $z = 0$ , which diverges at  $t \simeq 69$ . It is caused by the divergence of a quantity  $\dot{A}$ . We conclude a singularity forms at the origin  $z = 0$ .

This divergence is not a numerical error because a constraints equations (2.4) are always satisfied within  $10^{-5}$  -  $10^{-2}$  % accuracy except at time when the singularity appears.

In Appendix A, we study the reason why a spacetime is unstable and eventually evolves into a singularity in detail using a perturbation analysis of the Einstein equations and dynamical equation of  $\Phi$ . We find that a perturbed oscillation mode around an unperturbed kink solution becomes overstable for  $\kappa_5 = 0.1$ . From our analysis, we conclude that gravitational back reaction makes a kink solution unstable contrary to the Minkowski case.

Next, we show the result for the case of the initial velocity  $v = 0.2$ . In the Minkowski case, this incident velocity shows two-bounce at collision process (see Fig. 10 (a)). After two walls collide, they bounce, recede to some finite distance, turn back and then collide again.

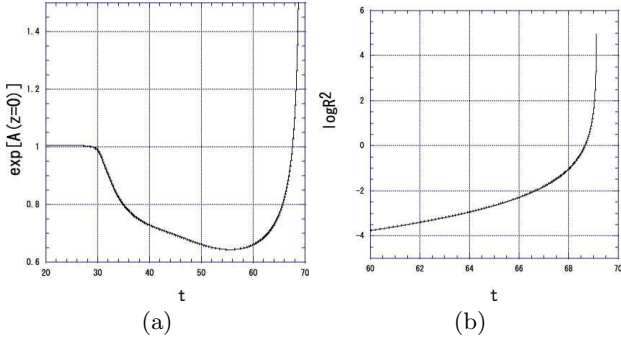


FIG. 9: (a) Time evolution of the metric component  $A$  at  $z = 0$  for  $v = 0.4$ ,  $d = \sqrt{2}$ ,  $\kappa_5 = 0.15$ . It diverges at  $t \sim 70$ . (b) Kretschmann scalar invariant ( $R^{abcd}R_{abcd}$ ) at the origin  $z = 0$  for the case of  $v = 0.4$ ,  $d = \sqrt{2}$ ,  $\kappa_5 = 0.15$ . We find that the Kretschmann scalar diverges at  $t \simeq 69$ . This means that it is not a coordinate singularity, but a curvature singularity.

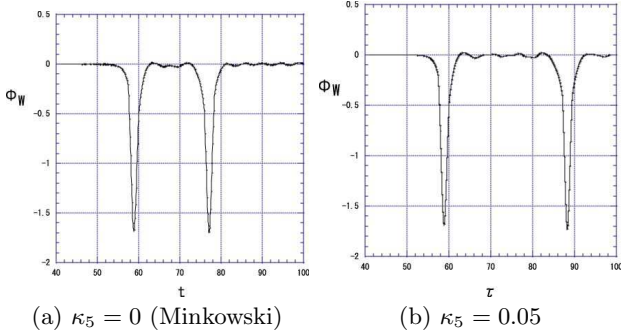


FIG. 10: Time evolution of a scalar field  $\Phi_W$  for  $v = 0.2$ ,  $d = \sqrt{2}$ . For (a)  $\kappa_5 = 0$  and (b)  $\kappa_5 = 0.05$ , we find two peaks which correspond to twice bounces at collision. Moreover, it is seen that an effective negative cosmological constant prolongs the time interval between two bounces.

For small values of  $\kappa_5$ , e.g.,  $\kappa_5 \leq 0.05$ , the collision process is very similar to the case of  $\kappa_5 = 0$  (see Fig. 10(b)). As  $\kappa_5$  increases, the time interval between first and second bounces becomes longer as shown in Fig. 11. This can be understood from the fact that the above mentioned oscillation after collision will radiate the energy. So a kink-antikink pair is loosely bounded and it takes longer time to collide again.

For the case of  $\kappa_5 \gtrsim 0.1$ , this feature of collision is drastically changed. Two-bounce collision never occurs, that is, two walls collide only once as shown in Fig. 12. This is because a lot of energy of a kink-antikink pair is radiated away via the unstable oscillation after collision and it has not enough energy to form a trapped state. After the first bounce, the domain walls never collide again but recede each other.

For larger value of  $\kappa_5$ , we find only one-bounce collision. Namely, a “negative cosmological constant” out-

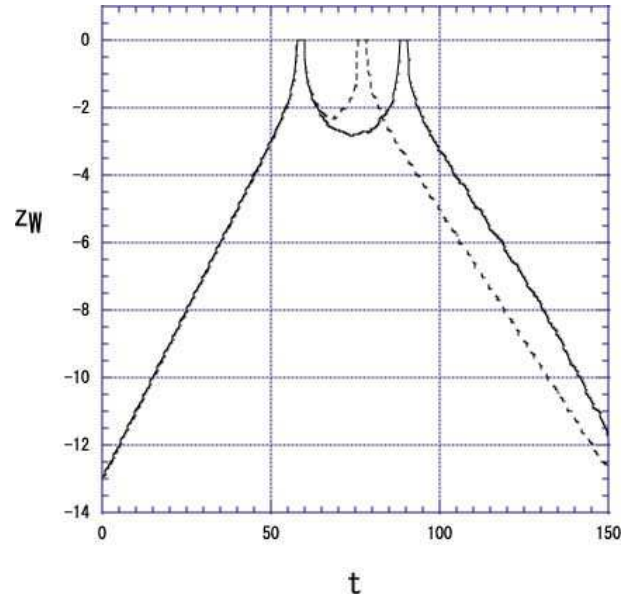


FIG. 11: Time evolution of the position of one brane  $z = z_W$  which starts to move at  $z = -13$  with a constant speed  $v = 0.2$ , setting  $d = \sqrt{2}$ ,  $\kappa_5 = 0.05$ . The dashed line denotes  $\kappa_5 = 0.05$  while the dotted line does  $\kappa_5 = 0$ . The time interval between two bounces is prolonged by an effective negative cosmological constant.

side a kink-antikink pair keeps away two walls toward the boundary, so it plays as an effective attractive force.

## B. Time Evolution of Metric

We evaluate the time evolutions of the metric  $A_W, B_W$  on the brane and plot them in Figs. 13. Both of two quantities decrease with time except that  $B_W$  increases slightly through the bounce.

From those two quantities, using Eqs. (3.4) and (3.5), we evaluate a scale factor of our universe  $a(\tau) = e^{B_W(\tau)}$  and the Hubble expansion parameter  $H \equiv \frac{da}{d\tau}/a$ , where  $\tau$  is the proper time of domain wall defined by Eq. (3.3), and show them in Figs. 14 setting  $v = 0.4$ . From this figure, we find that our universe expands slightly before bounce then eventually contracts. For each  $\kappa_5$ , the scale factor  $a$  and the Hubble parameter  $H$  are plotted in Figs. 15 and 16. From these figures, we see that our universe contracts faster as  $\kappa_5$  gets larger, i.e. a negative cosmological constant increases.

Next we investigate the scale factor  $a$  and the Hubble parameter  $H$  for the case of  $v = 0.2$ . Setting  $\kappa_5 = 0.05$ , that is the case of two-bounce collision,  $a$  and  $H$  are plotted in Fig. 17. We find two contracting phases, which correspond to each bounce at collision.

For  $\kappa_5 \gtrsim 0.1$ , the bounce occurs once only because of a large negative cosmological constant.  $a$  and  $H$  are plotted in Fig. 18 for  $\kappa_5 = 0.1$ . In this figure, we find the

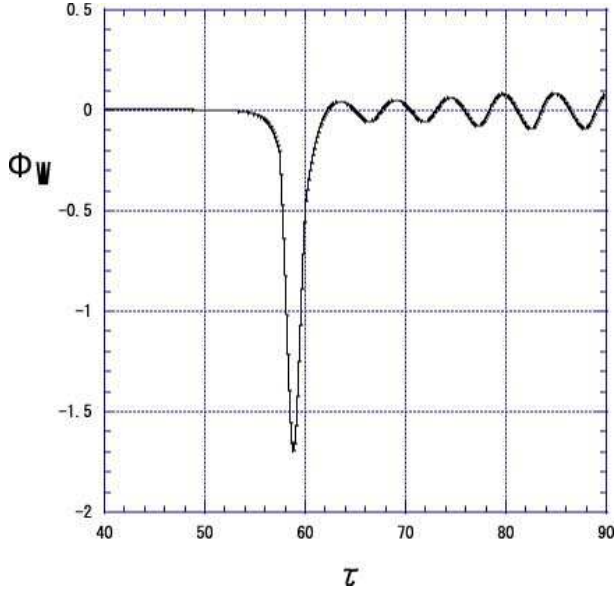


FIG. 12: Time evolution of the scalar field  $\Phi_W$  for  $v = 0.2$ ,  $d = \sqrt{2}$ ,  $\kappa_5 = 0.1$ . Two-bounce process does not occur. Compare it with the cases in Fig. 10.

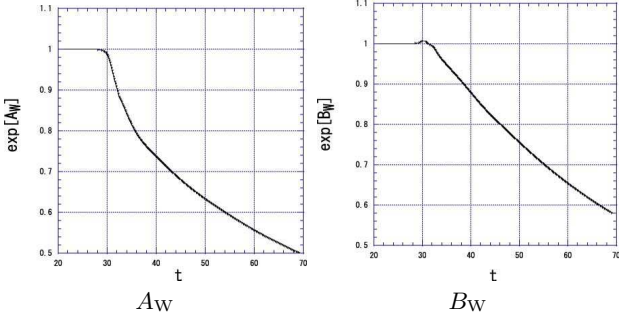


FIG. 13: Time evolution of the metric  $A$  and  $B$  on the moving wall for  $v = 0.4$ ,  $d = \sqrt{2}$ ,  $\kappa_5 = 0.15$ . The value of the metric is given by  $A_W = A(t, z_W(t))$ , where  $z_W(t)$  is the position of the wall. Both of two quantities decreases with time.

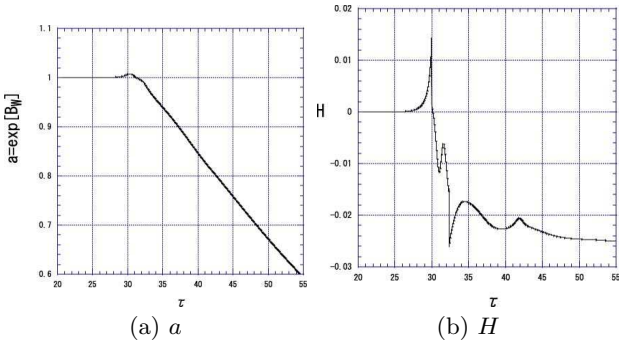


FIG. 14: Time evolution of the scale factor  $a = e^{B_W}$  and the Hubble parameter  $H \equiv \dot{a}(\tau)/a$  for  $v = 0.4$ ,  $d = \sqrt{2}$ ,  $\kappa_5 = 0.15$  with respect to the proper time  $\tau$ .

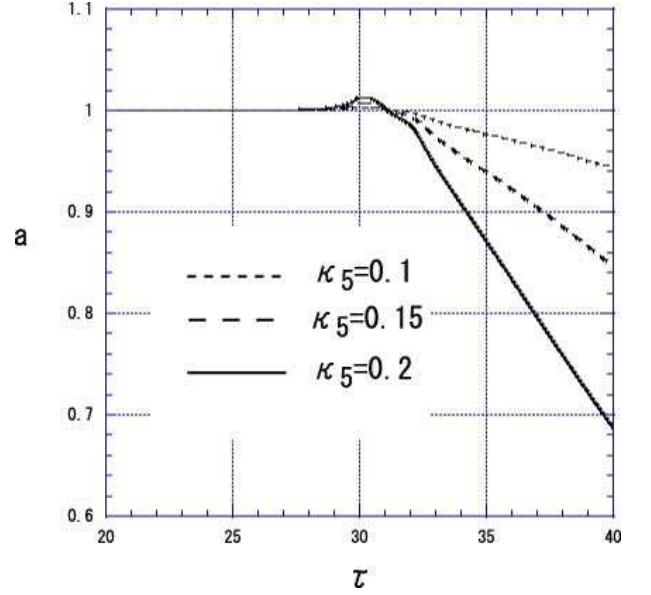


FIG. 15: Time evolution of the scale factor  $a = e^{B_W}$  for  $v = 0.4$ ,  $d = \sqrt{2}$ . We set  $\kappa_5 = 0.1, 0.15$  and  $0.2$ . As  $\kappa_5$  gets larger, the speed of contraction becomes larger.

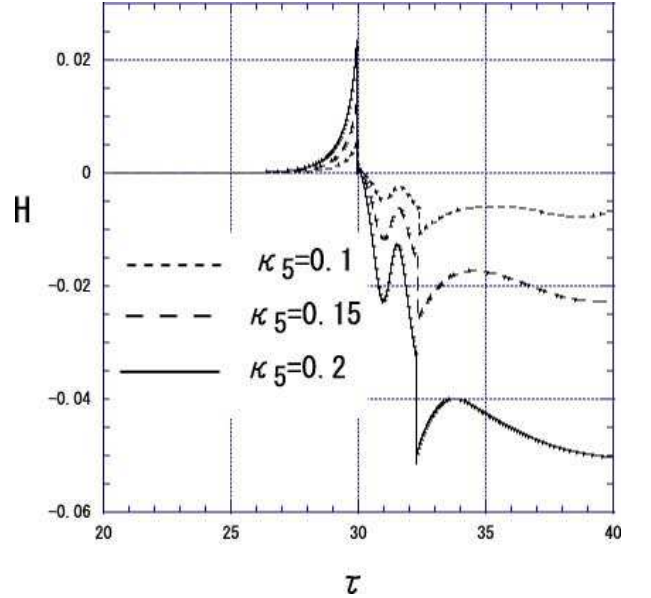


FIG. 16: Time evolution of the Hubble parameter  $H \equiv \dot{a}(\tau)/a$  for  $v = 0.4$ ,  $d = \sqrt{2}$ . We set  $\kappa_5 = 0.1, 0.15$  and  $0.2$ . As  $\kappa_5$  gets larger, the typical time scales of expansion and contraction become larger.

universe contracts slower than the case  $v = 0.4$ . Our universe contracts faster as  $v$  gets larger.

Finally, we find in Fig. 16 that there are two discontinuous stages in the evolution of the Hubble parameter at  $t \sim 30$  and  $\sim 32$ . As we will see, we can conclude that these discontinuities appear just because of ambiguity of

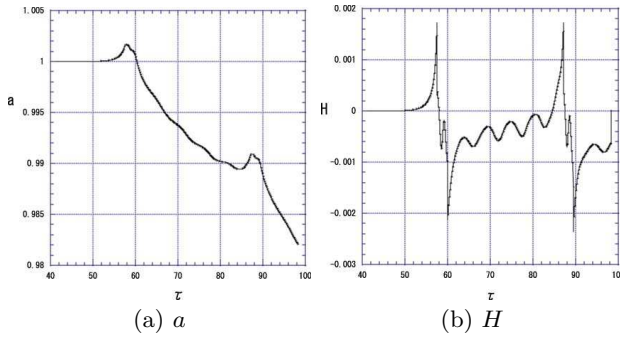


FIG. 17: Time evolution of the scalar factor  $a$  and the Hubble parameter  $H$  on the moving wall for  $v = 0.2$ ,  $d = \sqrt{2}$ ,  $\kappa_5 = 0.05$ . We find two contracting phases.

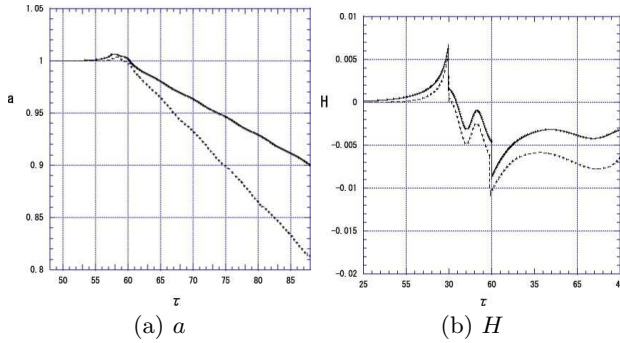


FIG. 18: Time evolution of the scalar factor  $a$  and the Hubble parameter  $H$  on the moving wall for  $v = 0.2$ ,  $d = \sqrt{2}$ ,  $\kappa_5 = 0.1$ . The dashed and dotted lines denote the cases of  $v = 0.2$  and of  $v = 0.4$ , respectively. We find the universe contracts slower in the case of  $v = 0.2$  than in the case  $v = 0.4$ .

the definition of a wall-position,  $z = z_W$ . The Hubble parameter mainly depends on the derivative of the metric with respect to  $t$ ,  $\dot{B}$ . This quantity in fact has two discontinuous stages as seen in Fig. 19. In this paper, we define the position of wall by one where the energy den-

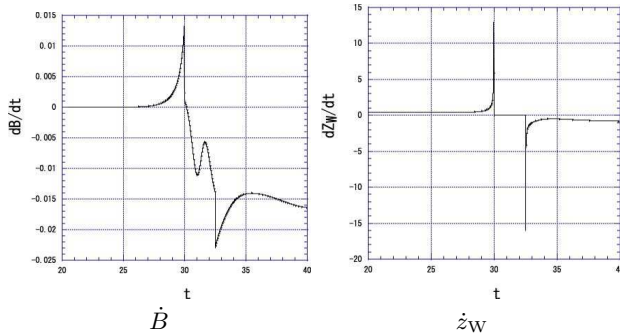


FIG. 19: Time evolution of  $\dot{B}$  and  $\dot{z}_W$  for  $v = 0.4$ ,  $d = \sqrt{2}$ ,  $\kappa_5 = 0.15$ . We find two discontinuous stages at  $t \sim 30$  and  $t \sim 32$ .

sity of scalar field gets maximum. However, this position does not move continuously through a bounce. Actually, we show  $\dot{z}_W$  has also two discontinuous stages as shown in Fig. 19, where the speed of a wall apparently exceeds the speed of light. Namely near the bounce, the definition of wall-position is not well-defined. This is because there is no wall configuration during the collision. Hence these discontinuities of the Hubble parameter seem to be apparent. We should look at the global time evolution.

#### IV. SUMMARY AND DISCUSSION

We have studied collision of two domain walls in 5D asymptotically Anti de Sitter spacetime. This may provide the reheating mechanism of an ekpyrotic (or cyclic) brane universe, in which two BPS branes collide and evolve into a hot big bang universe. We evaluate the values of both a scalar field corresponding to a domain wall and metric on the moving wall for different value of the warp factor  $k$  which is related to a gravitational effect  $\kappa_5$ . We analyze two typical incident velocities, i.e.  $v = 0.4$ , and  $v = 0.2$ , which correspond to one-bounce and two-bounce solutions in the Minkowski spacetime, respectively.

For the case of  $v = 0.4$ , the global feature of collision does not change so much for different values of  $\kappa_5$ , but the behaviour of oscillation after the collision is different for each  $\kappa_5$ . For small value of  $\kappa_5 \lesssim 0.01$ , the oscillation is the same as Minkowski case, but for  $\kappa_5 \gtrsim 0.05$ , it becomes an overstable oscillation. So its period and amplitude get larger as  $\kappa_5$  increases. In the cause of this unstable oscillation, the singularity appears after collision. This singularity is very similar to that found in Khan and Penrose [37], in which they discuss collision of plane waves and formation of a singularity. Hence the appearance of singularity in the present model could be understandable because we take into account a gravitational effect in collision of two domain walls.

In the time evolution of our universe, we find that the universe first expands a little just before collision and then contracts just after collision. This result is consistent with [28]. We cannot explain our hot big bang universe as it is. It is also found that the speed of expansion and contraction gets faster as  $\kappa_5$  increases.

For the second case, i.e.,  $v = 0.2$ , we show the bounce does not occur twice for larger value of  $\kappa_5$  ( $\kappa_5 \gtrsim 0.1$ ) corresponding to the unstable oscillation.

We shall discuss about the value of a warp factor  $k$ . We consider a curvature length  $l = 1/k$  written in the following form

$$l = 1.97 \times 10^{-17} \left( \frac{10^{-2}}{k} \right) \left( \frac{\text{TeV}}{m_\Phi} \right) [\text{m}], \quad (4.1)$$

where  $m_\Phi$  is a mass scale of a domain wall. Here we set a value of a warp factor  $k$  in the region  $0.01 \lesssim k \lesssim 0.25$ . On the other hand, we also know from the experimental data of testing a gravitational inverse-square law that the

curvature length must be smaller than 0.1 mm [38]. From this constraint equation, we obtain

$$k > 1.97 \times 10^{-15} \left( \frac{\text{TeV}}{m_\Phi} \right). \quad (4.2)$$

So the values of  $k$  used in our simulation satisfy this constraint.

### Acknowledgments

We would like to thank H. Kudoh and S. Mizuno for useful discussions. This work was partially supported by the Grant-in-Aid for Scientific Research Fund of the JSPS (No. 17540268) and another for the Japan-U.K. Research Cooperative Program, and by the Waseda University Grants for Special Research Projects and for The 21st Century COE Program (Holistic Research and Education Center for Physics Self-organization Systems) at Waseda University.

### APPENDIX A: PERTURBATIONS OF A DOMAIN WALL

In Fig. 6, we find oscillations after collision and those amplitudes and periods increase as  $\kappa_5$  gets larger. To understand this feature, we analyze perturbations around a static domain wall solution in this appendix.

We use the coordinate  $y$ , by which a static domain wall solution is given by analytically  $(\Phi_K(y), A_K(y))$ , which are given by Eqs. (2.7) and (2.9). We perturb the basic equations (2.3) and (2.4) by setting  $A = A_K(y) + a(t, y)$ ,  $B = A_K(y) + b(t, y)$ , and  $\Phi = \Phi_K(y) + \phi(t, y)$ . We find two sets of perturbation equations:

(1) dynamical equations

$$e^{-2A_K} \ddot{a} = \frac{\partial^2 a}{\partial y^2} + \frac{dA_K}{dy} \frac{\partial a}{\partial y} - 6 \frac{dA_K}{dy} \frac{\partial b}{\partial y} + \kappa_5^2 \left( 2 \frac{d\Phi_K}{dy} \frac{\partial \phi}{\partial y} - \frac{2}{3} V|_K a - \frac{1}{3} \frac{dV}{d\Phi} \Big|_K \phi \right), \quad (A1)$$

$$e^{-2A_K} \ddot{b} = \frac{\partial^2 b}{\partial y^2} + 7 \frac{dA_K}{dy} \frac{\partial b}{\partial y} + \frac{2}{3} \kappa_5^2 \left( 2V|_K a + \frac{dV}{d\Phi} \Big|_K \phi \right), \quad (A2)$$

$$e^{-2A_K} \ddot{\phi} = \frac{\partial^2 \phi}{\partial y^2} + 4 \frac{dA_K}{dy} \frac{\partial \phi}{\partial y} + 3 \frac{d\Phi_K}{dy} \frac{\partial b}{\partial y} - \frac{1}{2} \left( 2 \frac{dV}{d\Phi} \Big|_K a + \frac{d^2 V}{d\Phi^2} \Big|_K \phi \right), \quad (A3)$$

(2) constraint equations

$$\frac{\partial \dot{b}}{\partial y} - \frac{dA_K}{dy} \dot{a} = -\frac{2}{3} \kappa_5^2 \frac{d\Phi_K}{dy} \dot{\phi}, \quad (A4)$$

$$\frac{\partial^2 b}{\partial y^2} + 4 \frac{dA_K}{dy} \frac{\partial b}{\partial y} - \frac{dA_K}{dy} \frac{\partial a}{\partial y} + \frac{2}{3} \kappa_5^2 \left( V|_K a + \frac{1}{2} \frac{dV}{d\Phi} \Big|_K \phi + \frac{d\Phi_K}{dy} \frac{d\phi}{dy} \right) = 0 \quad (A5)$$

In order to find the eigenvalue and eigen functions, we set  $a = \tilde{a}(y)e^{i\omega t}$ ,  $b = \tilde{b}(y)e^{i\omega t}$ , and  $\phi = \tilde{\phi}(y)e^{i\omega t}$ . Then the constraint equation (A4) is reduced to be

$$\frac{d\tilde{b}}{dy} - \frac{dA_K}{dy} \tilde{a} = -\frac{2}{3} \kappa_5^2 \frac{d\Phi_K}{dy} \tilde{\phi} \quad (A6)$$

Inserting Eq. (A6) into another constraint (A5) and using the equations for a background solution, we find that the constraint equation (A5) turns out to be trivial. So we have only one constraint equation (A6).

Eliminating  $d\tilde{b}/dy$  in (A1) and (A3) by use of Eq. (A6), we obtain two coupled perturbation equations in terms of  $\tilde{a}, \tilde{\phi}$  as

$$\frac{d^2 \tilde{a}}{dy^2} = \left[ 6 \left( \frac{dA_K}{dy} \right)^2 + \frac{2}{3} \kappa_5^2 V|_K - e^{-2A_K} \omega^2 \right] \tilde{a} - \frac{dA_K}{dy} \frac{d\tilde{a}}{dy} - \kappa_5^2 \left( 4 \frac{dA_K}{dy} \frac{d\Phi_K}{dy} - \frac{1}{3} \frac{dV}{d\Phi} \Big|_K \right) \tilde{\phi} - 2 \kappa_5^2 \frac{d\Phi_K}{dy} \frac{d\tilde{\phi}}{dy}, \quad (A7)$$

$$\frac{d^2 \tilde{\phi}}{dy^2} = \left( \frac{dV}{d\Phi} \Big|_K - 3 \frac{d\Phi_K}{dy} \frac{dA_K}{dy} \right) \tilde{a} - 4 \frac{dA_K}{dy} \frac{d\tilde{\phi}}{dy} + \left[ 2 \kappa_5^2 \left( \frac{d\Phi_K}{dy} \right)^2 + \frac{1}{2} \frac{d^2 V}{d\Phi^2} \Big|_K - e^{-2A_K} \omega^2 \right] \tilde{\phi}. \quad (A8)$$

Eq. (A2) is guaranteed by the other two dynamical equations and constraint equations. Eqs. (A7) and (A8) have the asymptotic forms as  $y \rightarrow \infty$  as

$$\tilde{a} = e^{\pm \sqrt{A_1} y}, \quad (A9)$$

$$\tilde{\phi} = e^{\pm \sqrt{A_2} y}, \quad (A10)$$

where

$$A_1 = -e^{-2A_\infty} \omega^2, \quad (A11)$$

$$A_2 = \frac{1}{2} \frac{d^2 V}{d\Phi^2} \Big|_{\Phi=1} - e^{-2A_\infty} \omega^2. \quad (A12)$$

Here we choose both negative signs in Eqs. (A9) and (A10) because negative signs correspond to out-going wave modes.

We solve numerically these equations (A7, A8) connecting the above asymptotic solutions and find the complex eigen frequency  $\omega$ . For  $\kappa_5 = 0.1$ , we obtain a stable mode as  $\omega_s = 1.23 + 1.07 \times 10^{-3}i$  and unstable mode as  $\omega_u = 0.644 - 2.90 \times 10^{-2}i$ . Compared this unstable mode with the value obtained from the oscillations after collision found in Fig. 6 (Notice that we use a proper time  $\tau$  in Fig. 6. Then it should be evaluated in the physical time  $t$ ). We obtain  $0.772 \approx 1.2 \times \Re[\omega_u]$  for the real part of the frequency and  $-0.029 \approx 1.0 \times \Im[\omega_u]$  for the imaginary part. So we may conclude that the overstable oscillations after the collision of two domain walls found in Fig. 6 are explained by the unstable mode around a static domain wall solution.

- 
- [1] K. Sato, Mon. Not. Ray. Astron. Soc. **195**, 467 (1981); A. H. Guth, Phys. Rev. D **23**, 347 (1981); A. D. Linde, Phys. Lett. B **108**, 389 (1982); A. Albrecht and P. J. Steinhardt, Phys. Rev. Lett. **48**, 1220 (1982); A. A. Starobinsky, Phys. Lett. B **91**, 99 (1980).
- [2] For a review, see for example A. Linde, *Particle Physics and Inflationary Cosmology* (Harwood, Academic, Chur, Switzerland, 1990). E. W. Kolb and M. S. Turner, *The Early Universe* (Westview Press, Boulder, Colorado, 1990).
- [3] C. L. Bennett *et al.*, Astrophys. J. Suppl. **148** 1 (2003); G. Hinshaw *et al.*, *ibid.* **148** 135 (2003); D. N. Spergel *et al.*, *ibid.* **148** 175 (2003); H. V. Peiris *et al.*, *ibid.* **148** 213 (2003); A. Kogut *et al.*, *ibid.* **148** 161 (2003); E. Komatsu *et al.*, *ibid.* **148** 119 (2003).
- [4] S. Kachru, R. Kallosh, A. Linde, J. Maldacena, L. McAllister and S.P. Trivedi, JCAP **0310** 013 (2003).
- [5] K. Maeda and N. Ohta, Phys. Lett. B **597**, 400 (2004); K. Maeda and N. Ohta, Phys. Rev. D **71**, 063520 (2005).
- [6] K. Akama, Lect. Notes Phys. **176**, 267 (1982); V. A. Rubakov and M. E. Shaposhnikov, Phys. Lett. B **125**, 136 (1983); M. Visser, *ibid.* **159**, 22 (1985).
- [7] I. Antoniadis, Phys. Lett. B **246**, 377 (1990); N. Arkani-Hamed, S. Dimopoulos, and G. Dvali, *ibid.* **429**, 263 (1998); I. Antoniadis, N. Arkani-Hamed, S. Dimopoulos, and G. Dvali, *ibid.* **436**, 257 (1998).
- [8] J. Polchinski, Phys. Rev. Lett. **75**, 4724 (1995).
- [9] P. Hořava and E. Witten, Nucl. Phys. **B460**, 506 (1996); *ibid.* **B475**, 94 (1996).
- [10] J. Polchinski, *String Theory I & II* (Cambridge Univ. Press, Cambridge, 1998).
- [11] L. Randall and R. Sundrum, Phys. Rev. Lett. **83**, 3370 (1999).
- [12] L. Randall and R. Sundrum, Phys. Rev. Lett. **83**, 4690 (1999).
- [13] P. Binétruy, C. Deffayet and D. Langlois, Nucl. Phys. **B565**, 269 (2000); P. Binétruy, C. Deffayet, U. Ellwanger and D. Langlois, Phys. Lett. B **477**, 285 (2000).
- [14] C. Csaki, M. Graesser, C. Kolda and J. Terning Phys. Lett. B **462**, 34 (1999); N. Kaloper, Phys. Rev. D **60**, 123506 (1999); T. Nihei, Phys. Lett. B **465**, 81 (1999); H. S. Reall, Phys. Rev. D **59**, 103506 (1999).
- [15] A. Lukas, B. A. Ovrut, K. S. Stelle, and D. Waldram, Phys. Rev. D **59**, 086001 (1999); A. Lukas, B. A. Ovrut, and D. Waldram, *ibid.* **60** 086001 (1999).
- [16] K. Maeda, Prog. Theor. Phys. Suppl. **148**, 59 (2003); K. Maeda, Lect. Notes Phys. **646**, 323 (2004).
- [17] R. Maartens, arXiv:gr-qc/0101059; R. Maartens, Prog. Theor. Phys. Suppl. **148**, 213 (2003); R. Maartens, arXiv:gr-qc/0312059.
- [18] D. Langlois, arXiv:gr-qc/0207047; D. Langlois, Prog. Theor. Phys. Suppl. **148**, 181 (2003).
- [19] P. Brax and C. van de Bruck, Class. Quant. Grav. **20**, 201R (2003); P. Brax, C. van de Bruck and A. C. Davis, arXiv:hep-th/0404011.
- [20] T. Shiromizu, K. Maeda, and M. Sasaki, Phys. Rev. D **62**, 024012 (2000); S. Mukohyama, T. Shiromizu and K. Maeda, *ibid.* D **62**, 024028 (2000).
- [21] K. Maeda and D. Wands, Phys. Rev. D **62**, 124009 (2000).
- [22] J. Khoury, B. A. Ovrut, P. J. Steinhardt and N. Turok, Phys. Rev. D **64**, 123522 (2001); J. Khoury, B. A. Ovrut, N. Seiberg, P. J. Steinhardt and N. Turok, *ibid.* **65**, 086007 (2002); J. Khoury, B. A. Ovrut, P. J. Steinhardt and N. Turok, *ibid.* **66**, 046005 (2002); A. J. Tolley and N. Turok, *ibid.* **66**, 106005 (2002).
- [23] P. J. Steinhardt and N. Turok, Phys. Rev. D **65**, 126003 (2002); J. Khoury, P. J. Steinhardt and N. Turok, Phys. Rev. Lett. **92**, 031302 (2004).
- [24] D. H. Lyth, Phys. Lett. B **524**, 1 (2002).
- [25] R. Brandenberger and F. Finelli, J. High Energy Phys. **111**, 056 (2001); F. Finelli and R. Brandenberger, Phys. Rev. D **65**, 103522 (2002).
- [26] J. Martin, P. Peter, N. Pinto Neto and D. J. Schwarz, Phys. Rev. D **65**, 123513 (2002); P. Peter and N. Pinto-Neto, *ibid.* **66**, 063509 (2002); J. Martin, P. Peter, N. Pinto-Neto and D. J. Schwarz, *ibid.* **67**, 028301 (2003).
- [27] S. Tsujikawa, Phys. Lett. B **526**, 179 (2002); S. Tsujikawa, R. Brandenberger and F. Finelli, Phys. Rev. D **66**, 083513 (2002); L. E. Allen and D. Wands, *ibid.* **70** 063515 (2004).
- [28] D. Langlois, K. Maeda, and D. Wands Phys. Rev. Lett. **88** 181301 (2002).
- [29] J. Martin, G. N. Felder, A. V. Frolov, M. Peloso and L. Kofman, Phys. Rev. D **69**, 084017 (2004); J. Martin, G. N. Felder, A. V. Frolov, L. Kofman and M. Peloso, Comput. Phys. Commun. **171** 69 (2005).
- [30] J.M. Cline, H. Firouzjahi and P. Martineau, J. High Energy Phys. **211**, 041 (2002); N. Barnaby and J. M. Cline, Phys. Rev. D **70** 023506 (2004).
- [31] Y. Takamizu and K. Maeda, Phys. Rev. D **70**, 123514 (2004).
- [32] P. Anninos, S. Oliveira and R. A. Matzner, Phys. Rev. D **44**, 1147 (1991).
- [33] V. Silveira, Phys. Rev. D **38**, 3823 (1988).
- [34] T. I. Belova and A. E. Kudryavtsev, Physica D **32**, 18 (1988).
- [35] D. K. Campbell, J. F. Schonfeld and C. A. Wingate, Physica D (Amsterdam) **9**, 1 (1983).
- [36] M. Eto and N. Sakai, Phys. Rev. D **68**, 125001 (2003).
- [37] K. A. Khan and R. Penrose, Nature **229**, 185 (1971).
- [38] J. C. Long, H. W. Chan and J. C. Price, Nucl. Phys. **B539** 23 (1999); C. D. Hoyle, U. Schmidt, B. R. Heckel, E. G. Adelberger, J. H. Gundlach, D. J. Kapner and H. E. Swanson, Phys. Rev. Lett. **86** 1418 (2001); E. G. Adelberger, B. R. Heckel and A. E. Nelson, Ann. Rev. Nucl. Part. Sci. **53** 77 (2003).